PHYSICAL REVIEW B **71**, 220103(R) (2005)

Bulk modulus anomaly in $R\mathrm{CoO_3}$ (R=La, Pr, and Nd)

J.-S. Zhou, J.-Q. Yan,* and J. B. Goodenough
Texas Materials Institute, 1 University Station, C2201, University of Texas, Austin, Texas 78712, USA
(Received 17 March 2005; published 23 June 2005)

In order to demonstrate the effect of hydrostatic pressure and chemical pressure on crystal structure and the spin-state transition in the perovskites $R\mathrm{CoO_3}$ (R=La, Pr, and Nd), x-ray diffraction has been carried out under pressure up to 80 kbar. A sharp difference of the bulk modulus found between the higher-spin $\mathrm{LaCoO_3}$ and $\mathrm{PrCoO_3}$ and the low-spin $\mathrm{NdCoO_3}$ has been interpreted to reflect a pressure-induced spin-state transition in $\mathrm{LaCoO_3}$ and $\mathrm{PrCoO_3}$. A change in the bandwidth of the σ bonding electrons due to the structural distortion has been shown to be the driving force for the spin-state transition caused by chemical pressure. On the other hand, the changes in this bandwidth must be overcompensated by the cubic-field splitting resulting from a shorter Co–O bond length in order to account for the spin-state transition under hydrostatic pressure.

DOI: 10.1103/PhysRevB.71.220103 PACS number(s): 61.50.Ks, 75.25.+z

In the $R\mathrm{CoO_3}$ (R=rare earth) perovskite family, the energy difference $(\Delta_c-\Delta_{ex})$ between the cubic crystal-field splitting and the intra-atomic Hund exchange-field splitting at the octahedral-site Co(III) ions is small, i.e., comparable to kT at room temperature, which makes the spin state of the Co(III) ions extremely sensitive to temperature, chemical pressure, hydrostatic pressure, and subtle changes in the crystal structure. With increasing temperature, $\mathrm{LaCoO_3}$ exhibits a progressive transition from the low-spin (LS) state Co(III): t^6e^0 to a higher-spin state $t^{6-\delta}e^{\delta}$ ($\delta>0$), and the intermediate-spin (IS) state t^5e^1 is dominant at 300 K.[1–3] Therefore, the observation of an unusually low bulk modulus for $\mathrm{LaCoO_3}$ compared to that of other $RM\mathrm{O_3}$ perovskites was interpreted to reflect a pressure-induced IS to LS transition.[4] The bulk LS phase of $\mathrm{LaCoO_3}$ was reported to be stabilized at room temperature in pressures $P>4$ GPa.

Substitution for La^{3+} of an R^{3+} ion of smaller ionic radius (IR) introduces a chemical pressure on the $\mathrm{CoO_3}$ array, but a geometrical tolerance factor $t\equiv(R-\mathrm{O})/\sqrt{2}(\mathrm{Co–O})<1$, where $(R-\mathrm{O})$ and $(\mathrm{Co—O})$ are equilibrium bond lengths, allows cooperative $\mathrm{CoO_{6/2}}$ site rotations that relieve the compressive stress on the Co–O bond. Consequently, the LS Co–O bond length changes little with IR. Nevertheless, the onset temperature for the transition from the LS state ($\delta=0$) to a higher-spin state ($\delta>0$) at the Co(III) ions increases with decreasing IR.[3,5] In this paper we argue that this apparent increase in $(\Delta_c-\Delta_{ex})$ with decreasing IR cannot be attributed to a shorter Co–O bond length as occurs under hydrostatic pressure, so we are forced to look for an alternative explanation.

The cooperative $M\mathrm{O_{6/2}}$ site rotations in $RM\mathrm{O_3}$ perovskites bend the $M-\mathrm{O}-M$ bond angles from 180° to $(180°-2\omega)$; this bending, which reduces the strength of the interatomic $M-\mathrm{O}-M$ interactions, can trigger an electronic transition as occurs in the $R\mathrm{NiO_3}$ family.[6] The cooperative site rotations give rise to a sequence of structural symmetry changes with increasing IR from orthorhombic to rhombohedral to tetragonal to cubic with decrease in the bending angle ω. The tolerance factor t of the $R^{3+}M^{3+}\mathrm{O_3}$ perovskites increases under hydrostatic pressure.[7] Therefore, hydrostatic pressure increases t whereas chemical pressure (smaller IR) decreases t, but both pressures increase the effective $(\Delta_c-\Delta_{ex})$ in the $R\mathrm{CoO_3}$ family. In order to clarify this seeming paradox, we have carried out a room-temperature structural study of the $R\mathrm{CoO_3}$ perovskites under pressure for R=La, Pr, Nd. These selected members of the $R\mathrm{CoO_3}$ family exhibit different concentrations of higher-spin Co(III) ions at room temperature, and there is a structural transition from the rhombohedral phase in $\mathrm{LaCoO_3}$ to the orthorhombic phase in $\mathrm{PrCoO_3}$.

Powder samples of $R\mathrm{CoO_3}$ were made by crushing single-crystal ingots that had been grown in an infrared-heating image furnace. The oxygen stoichiometry of these samples was checked by measuring the thermoelectric power. Rectangular bars cut from these ingots were used previously to measure the thermal conductivity and magnetic susceptibility;[3] these data showed the onset temperature from the LS state to a higher-spin state increases from ~35 K in $\mathrm{LaCoO_3}$ to ~200 K in $\mathrm{PrCoO_3}$ and to ~300 K in $\mathrm{NdCoO_3}$. The x-ray diffraction (XRD) under high pressure was carried out with a diamond-anvil cell; $\mathrm{CaF_2}$ (Ref. 8) and a 4:1 mixture of methanol and ethanol were used, respectively, as the pressure manometer and the pressure medium. Application of a monocapillary collimator improved the beam intensity from a 2-kW fine-focus Mo anode tube. The XRD pattern was collected on a Fuji image plate that was scanned and digitized with a Fuji image-plate scanner BAS1800 II. The image profile was integrated to a two-column data of intensity vs 2θ with the software FIT2D, and lattice parameters were obtained by least-square fitting with the software JADE.

Effect of pressure on the structure. The distortion from cubic to orthorhombic symmetry in the $RM\mathrm{O_3}$ perovskites is due to a cooperative rotation of the $M\mathrm{O_{6/2}}$ octahedra about the b axis in space group $Pbnm$, which makes $b>a$. However, we[9] have recently shown unambiguously that as the IR increases to beyond a critical value, a distortion of the $M\mathrm{O_{6/2}}$ sites from cubic symmetry is added to their cooperative rotation, and this site distortion inverts $b>a$ to $a>b$ before the perovskite transforms from orthorhombic $Pbnm$ to rhombohedral $R\bar{3}c$ symmetry; in the $R\bar{3}c$ structure, the cooperative $M\mathrm{O_{6/2}}$-site rotations are about the [111] axis. The $R\mathrm{CoO_3}$ family is one of the few that exhibits the $Pbnm$ to $R\bar{3}c$ cross-

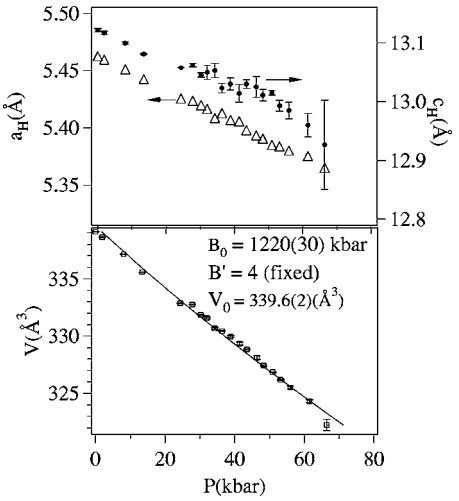

FIG. 1. Pressure dependence of lattice parameters for rhombohedral $LaCoO_3$. The hexagonal cell is used to index the rhombohedral phase. The pressure dependence of volume was fitted to the BM equation with fitting parameters labeled inside the figure.

over with increasing IR; $LaCoO_3$ has rhombohedral symmetry and a $b>a$ in orthorhombic $NdCoO_3$ changes to $a>b$ in orthorhombic $PrCoO_3$. We first examine whether the $RCoO_3$ structure evolves with increasing tolerance factor under hydrostatic pressure in the same way it does under reducing chemical pressure.

As shown in Fig. 1, the rhombohedral phase of $LaCoO_3$ is stable to the highest pressures used in this work. Figure 2 shows the lattice-parameter order $a>b$ in orthorhombic $PrCoO_3$ is retained until $P\approx 45$ kbar, where a first-order transition to the rhombohedral phase takes place. Figure 3 shows a crossover from $b>a$ to $a>b$ at $P\approx 10$ kbar in orthorhombic $NdCoO_3$ and an increase to $P\approx 64$ kbar in the

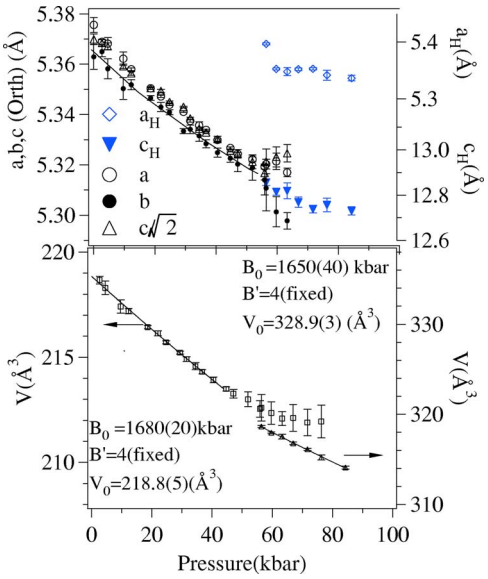

FIG. 2. Pressure dependence of lattice parameters for orthorhombic $PrCoO_3$. The two-phase region near $P=50$ kbar indicates the first-order character of the orthorhombic-rhombohedral phase transition.

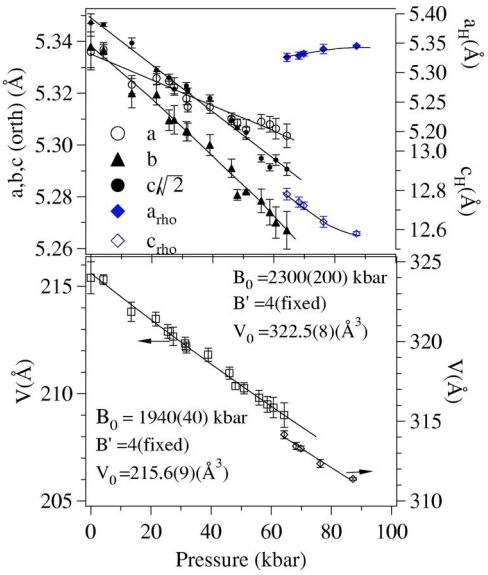

FIG. 3. The same as Fig. 2 for $NdCoO_3$.

pressure of the orthorhombic to rhombohedral transition. The structural evolution induced by hydrostatic pressure duplicates precisely what is found as the IR increases.

Effect of pressure on the spin state. Probing the spin-state transition on the Co(III) ions under chemical or hydrostatic pressure is not as straightforward as monitoring the structural changes since no specific structural change is associated with the spin-state transition[10] and this transition is progressive. However, thermal conductivity and magnetic susceptibility measurements[3] have shown that at room temperature the Co(III)-ion spin state is predominantly LS in $NdCoO_3$ and predominantly IS in $LaCoO_3$; $PrCoO_3$ has a smaller concentration of IS Co(III) than $LaCoO_3$.

The schematic one-electron energy diagram of Fig. 4(a) for the π-bonding t and σ-bonding e states in an octahedral site illustrates the subtle balance between the cubic-field splitting Δ_c and the intra-atomic exchange splitting Δ_{ex} at the Co(III) ions in the $RCoO_3$ perovskites. The difference in the effective $(\Delta_c-\Delta_{ex})$ may be altered by the introduction of a Jahn-Teller site distortion, which stabilizes predominantly the IS state t^5e^1 relative to the high-spin (HS) state t^4e^2 in $LaCoO_3$ at 300 K. However, the bandwidth W resulting from the σ-bonding Co–O–Co interactions and the cubic-field splitting Δ_c are the dominant factors to be considered in any comparison of the influences of chemical or hydrostatic pressure on the effective $(\Delta_c-\Delta_{ex})$, i.e., on $(\Delta_c-W/2-\Delta_{ex})$. From Fig. 4(a), it is clear that broadening W favors stabilization of a higher-spin state; and the bandwidth is given by[11,12] $W\sim\cos\omega/(\text{Co–O})$,[3,5] where ω is defined in the inset of Fig. 4(a). Figure 4(b) shows that the $(M-\text{O})$ bond length varies little with IR in the perovskites $RFeO_3$ and $RMnO_3$ where there is no change in the spin state; it is the bending angle ω that decreases systematically with increasing IR. The principle effect of chemical pressure is to buckle the MO_3 array. These two examples show truly the effect of chemical pressure on the M–O bond length. In the $RCoO_3$ family, the fraction of higher-spin Co(III) at 300 K increases monotonically on going from R=Nd to Pr to La, which causes some

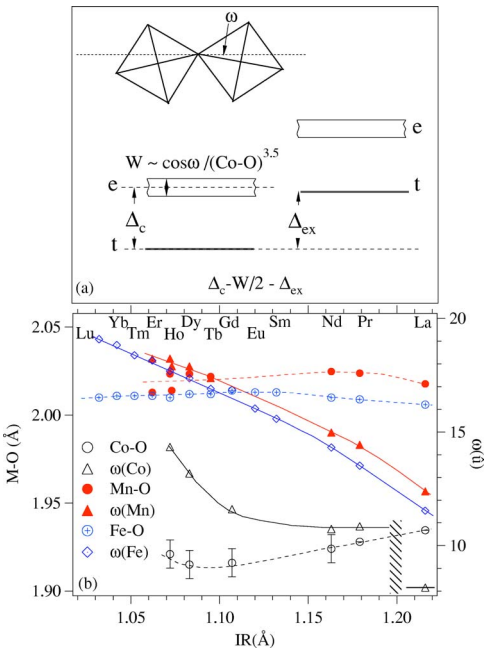

FIG. 4. (a) Schematic one-electron d-orbital energies for RCoO$_3$, including a σ^* bandwidth W and a definition of the tilting angle ω. (b) The tilting angle ω and $M-$O bond length vs the ionic size of the R^{3+} ion (IR), which is that tabulated for nine coordination, for RFeO$_3$ (Refs. 21 and 22), RMnO$_3$ (Refs. 13 and 23), and RCoO$_3$ [R=La (Ref. 24), Pr (Ref. 25), the rest (Ref. 26)]. The Mn–O and Co–O bond lengths shown in the figure are the average value. The neutron diffraction data are available only for the RCoO$_3$ (R=La,Pr). Since they were obtained through the refinement of x-ray powder diffraction, the error bars and systematic error in the tilting angle ω for the RCoO$_3$ (R=Nd, Gd, Dy, and Ho) are so large that the real difference $\Delta\omega$ between PrCoO$_3$ and NdCoO$_3$ cannot be resolved in the figure.

increase in the average (Co—O) bond length. However, we emphasize that this change in the equilibrium Co—O bond length is a consequence of the spin-state transition; it is *not* the driving force for this transition. We also point out that the bending angle ω drops discontinuously across the transition from orthorhombic to rhombohedral symmetry.

In contrast to the lattice response to chemical pressure (smaller IR), hydrostatic pressure reduces both the ($M-$O) bond length and the bending angle ω as has been shown in LaMnO$_3$,[13] GdFeO$_3$,[14] and PrNiO$_3$.[11] Therefore, hydrostatic pressure not only increases Δ_c by shortening the ($M-$O) bond length; it also broadens the bandwidth W, which would stabilize a higher-spin state. Therefore, we must look to experiments to determine how the system deals with this competition. An anomalously small room-temperature bulk modulus found for LaCoO$_3$ led Vogt *et al.*[4] to conclude that the LS state is stabilized by hydrostatic pressure in this compound; the higher-spin Co(III): $t^{6-\delta}e^{\delta}$ ions achieve a shorter equilibrium (Co–O) bond length by transferring their σ-bond e electrons to π-bonding t orbitals. On the other hand, an inverse pressure effect has been observed near the boundary of localized to itinerant electronic behavior in Sr-doped LaCoO$_3$.[15,16] Sr doping in La$_{1-x}$Sr$_x$CoO$_3$ stabilizes a higher-spin state $t^6\sigma^{*(1-x)}$ in which the e electrons occupy itinerant-electron states in a σ^* band of e-orbital parentage.[17–19] The transformation from localized $-e$ to itinerant $-\sigma^*$ states broadens significantly the bandwidth W of the σ-bonding e states, and this broadening overcomes any enlarged cubic-field splitting at the pressures employed.

Fitting the curve of volume versus pressure for LaCoO$_3$, Fig. 1(b), to the Birch-Murnaghan (BM) equation

$$P = \frac{3B_0}{2}\left[\left(\frac{V_0}{V}\right)^{7/3} - \left(\frac{V_0}{V}\right)^{5/3}\right]\left\{1 + \frac{3}{4}(B' - 4)\left[\left(\frac{V_0}{V}\right)^{2/3} - 1\right]\right\}$$

gives an even lower bulk modulus, B_o=1220(30) kbar, than that reported by Vogt *et al.*[4] We found no clear evidence that the transition to all LS Co(III) is completed by 70 kbar. The continuous character of the transition from the higher-spin to the LS state under pressure makes the best fit to the $V(P)$ curve with $B' \approx 1$ in the BM equation, which deviates significantly from a value B'=4–6 typical of an elastic lattice.

PrCoO$_3$ has a smaller concentration of high-spin Co(III) at room temperature than LaCoO$_3$. The increase in the effective ($\Delta_c - \Delta_{ex}$) can be attributed to the larger bending of the Co–O–Co bonds in PrCoO$_3$, which narrows the σ^* bandwidth W. Fitting the curve of Fig. 2(b) to the BM equation with B'=4 gives B_o=1680(20) kbar in the orthorhombic ($\mathcal{O}$) phase ($P<45$ kbar) and B_o=1650(40) kbar in the rhombohedral ($\mathcal{R}$) phase ($P>55$ kbar). LaGaO$_3$ undergoes a similar $\mathcal{O}$-$\mathcal{R}$ transition under pressure; but in contrast, it has a higher B_o in its $\mathcal{R}$ phase than in its $\mathcal{O}$ phase.[20] The bending angles ω are reduced discontinuously on crossing from $\mathcal{O}$ to $\mathcal{R}$ symmetry. Therefore, the σ^* bandwidth W of PrCoO$_3$ is larger in the $\mathcal{R}$ phase, which decreases the effective ($\Delta_c - \Delta_{ex}$) so as to increase the population of higher-spin Co(III). A greater population of higher-spin Co(III) lowers B_o towards its value in LaCoO$_3$.

NdCoO$_3$ contains few higher-spin Co(III) at room temperature, so we can expect a higher B_o more in line with other RMO_3 perovskties as well as an increase in B_o on crossing from the $\mathcal{O}$ to the $\mathcal{R}$ phase as in LaGaO$_3$. Figure 3(b) shows that this expectation is indeed realized in NdCoO$_3$. On the other hand, the increase in B_o on going from isostructural PrCoO$_3$ to NdCoO$_3$ could be argued to be due to an intrinsic change caused by a larger bending angle ω. Zhao *et al.*[7] have recently shown that the B_o of AMO_3 perovskites depends primarily on the ratio of the compressibilities of the ($A-$O) and ($M-$O) bonds and only weakly on the elements A and M. They have further derived a relationship between this ratio, which is difficult to determine experimentally, and the ratio of bond-valence parameters that can be calculated from the crystal structure. Using their empirical relationship and calculated bond-valence parameters, we have obtained a maximum increase in B_o between PrCoO$_3$ and NdCoO$_3$ due to the increased bond bending to be 3%, which is too small to account for the 15% jump in B_o observed experimentally from Figs. 2(b) and 3(b). This comparison confirms unambiguously that the unusually low values of B_o found in LaCoO$_3$ and PrCoO$_3$ are caused by the progressive pressure-induced transfer of e electrons to t orbitals in the Co(III)O$_3$ array. In conclusion, hydrostatic pressure increases the tolerance factor t and chemical pressure

(smaller IR) reduces it, but both stabilize the LS state relative to a higher-spin state by increasing the effective energy difference $(\Delta_c - \Delta_{ex})$, i.e., $(\Delta_c - W/2 - \Delta_{ex})$. Chemical pressure increases the bending of the $(180° - 2\omega)$ Co–O–Co bond angle without changing significantly the LS Co(III)–O equilibrium bond length. In this case, the effective $(\Delta_c - \Delta_{ex})$ is increased by a narrowing of the σ^* bandwidth $W \sim \cos\omega/(\mathrm{Co—O})^{3.5}$. On the other hand, hydrostatic pressure decreases both the (Co–O) bond length and the bending of the Co–O–Co bond. Both effects increase W, but a decreased (Co–O) bond length increases Δ_c. A bulk modulus B_o typical of that for other RMO_3 perovskites has been found for $NdCoO_3$, which has few higher-spin Co(III) at room temperature; but $LaCoO_3$ and $PrCoO_3$ have much smaller values of B_o, and the reduction in B_o increases with the population of higher-spin Co(III) at room temperature. Therefore, a pressure-induced relative stabilization of the LS state can be inferred from the compressibility. It follows that the increase in Δ_c under hydrostatic pressure must be greater than the increase in $W/2$.

We thank the NSF and the Robert A. Welch Foundation, Houston, TX, for financial support.

---

*Present address: Ames Laboratory, Neutron and X-ray Group, A524 Physics, Ames, IA 50011.

[1] J. B. Goodenough, J. Chem. Phys. **6**, 287 (1958).
[2] K. Asai, A. Yoneda, O. Yokokura, J. M. Tranquada, G. Shirane, and K. Kohn, J. Phys. Soc. Jpn. **67**, 290 (1998).
[3] J.-Q. Yan, J.-S. Zhou, and J. B. Goodenough, Phys. Rev. B **69**, 134409 (2004).
[4] T. Vogt, J. A. Hriljac, N. C. Hyatt, and P. Woodward, Phys. Rev. B **67**, 140401(R) (2003).
[5] J. Baier, S. Jodlauk, M. Kriener, A. Reichl, C. Zobel, H. Kierspel, A. Freimuth, and T. Lorenz, Phys. Rev. B **71**, 014443 (2005).
[6] J.-S. Zhou and J. B. Goodenough, Phys. Rev. B **69**, 153105 (2004).
[7] J. Zhao, N. L. Ross, and R. J. Angel, Acta Crystallogr., Sect. B: Struct. Sci. **60**, 263 (2004).
[8] R. J. Angel, J. Phys.: Condens. Matter **5**, L141 (1993).
[9] J.-S. Zhou and J. B. Goodenough, Phys. Rev. Lett. **94**, 065501 (2005).
[10] Sheng Xu and Yutaka Moritomo, J. Phys. Soc. Jpn. **70**, 3296 (2001).
[11] M. Medarde, J. Mesot, P. Lacorre, S. Rosenkranz, P. Fischer, and K. Gobrecht, Phys. Rev. B **52**, 9248 (1995).
[12] W. A. Harrison, *The Electronic Structure and Properties of Solids* (Freeman, San Francisco, 1980).
[13] L. Pinsard-Gaudart, J. Rodriguez-Carvajal, A. Daoud-Aladine, I. Goncharenko, M. Medarde, R. I. Smith, and A. Revcolevschi, Phys. Rev. B **64**, 064426 (2001).
[14] N. L. Ross, J. Zhao, J. B. Burt, and T. D. Chaplin, J. Phys.: Condens. Matter **16**, 5721 (2004).
[15] R. Lengsdorf, M. Ait-Tahar, S. S. Saxena, M. Ellerby, D. I. Khomskii, H. Micklitz, T. Lorenz, and M. M. Abd-Elmeguid, Phys. Rev. B **69**, 140403(R) (2004).
[16] I. Fita, R. Szymczak, R. Puzniak, I. O. Troyanchuk, J. Fink-Finowicki, Ya. M. Mukovskii, V. N. Varyukhin, and H. Szymczak, Phys. Rev. B **71**, 214404 (2005).
[17] J. B. Goodenough, Mater. Res. Bull. **6**, 967 (1971).
[18] M. A. Senaris-Rodriguez and J. B. Goodenough, J. Solid State Chem. **118**, 323 (1995).
[19] D. Louca, J. L. Sarrao, J. D. Thompson, H. Roder, and G. H. Kwei, Phys. Rev. B **60**, 10378 (1999).
[20] B. J. Kennedy, T. Vogt, C. D. Martin, J. B. Parise, and J. A. Hriljac, J. Phys.: Condens. Matter **13**, L925 (2001).
[21] M. Marezio and P. D. Dernier, Mater. Res. Bull. **6**, 23 (1971).
[22] M. Marezio, J. P. Remeika, and P. D. Dernier, Acta Crystallogr. **26**, 2008 (1970).
[23] J. A. Alonso, M. J. Martinez-Lope, M. T. Casais, and M. T. Fernandez-Diaz, Inorg. Chem. **39**, 917 (2000).
[24] P. G. Radaelli and S.-W. Cheong, Phys. Rev. B **66**, 094408 (2002).
[25] Y. Ren, J.-Q. Yan, J.-S. Zhou, S. Short, J. D. Jorgensen, and J. B. Goodenough (unpublished).
[26] X. Liu and C. T. Prewitt, J. Phys. Chem. Solids **52**, 441 (1991).